

# Thermal relaxation and low-frequency vibrational anomalies in simple models of glasses: A study using nonlinear Hamiltonians

J. R. Romero-Arias

*Instituto de Física, Departamento de Física-Química, Universidad Nacional Autónoma de México (UNAM),  
Apartado Postal 20-364, 01000, Distrito Federal, Mexico*

Gerardo G. Naumis\*

*Facultad de Ciencias, Universidad Autónoma del Estado de Morelos, Av. Universidad 1001, Colonia Chamilpa, 62210 Cuernavaca,  
Morelos, México and Departamento de Física-Matemática, Universidad Iberoamericana,  
Prolongación Paseo de la Reforma 880, Colonia Lomas de Santa Fe 01210, Distrito Federal, Mexico,*

(Received 14 January 2008; published 5 June 2008)

Glasses exist because they are not able to relax in a laboratory time scale toward the most stable structure: a crystal. At the same time, glasses present low-frequency vibrational-mode (LFVM) anomalies. We explore in a systematic way how the number of such modes influences thermal relaxation in one-dimensional models of glasses. The model is a Fermi-Pasta-Ulam chain with nonlinear springs that join second neighbors at random, which mimics the adding of bond constraints in the rigidity theory of glasses. The corresponding number of LFVMs decreases linearly with the concentration of these springs, and thus their effect upon thermal relaxation can be studied in a systematic way. To do so, we performed numerical simulations using lattices that were thermalized and afterwards placed in contact with a zero-temperature bath. The results indicate that the time required for thermal relaxation has two contributions: one depends on the number of LFVMs and the other on the localization of modes due to disorder. By removing LFVMs, relaxation becomes less efficient since the cascade mechanism that transfers energy between modes is stopped. On the other hand, normal-mode localization also increases the time required for relaxation. We prove this last point by comparing periodic and nonperiodic chains that have the same number of LFVMs.

DOI: [10.1103/PhysRevE.77.061504](https://doi.org/10.1103/PhysRevE.77.061504)

PACS number(s): 64.70.Q-, 64.70.kj, 05.45.-a, 63.20.Ry

## I. INTRODUCTION

After many years of research, glass formation still remains as a source of debate in the scientific community [1]. The main reason is the nonequilibrium nature of the process. As a consequence, some important questions concerning glass science and technology are unanswered [2]. Among these we can cite the origin of the nonexponential relaxation laws [3] or why certain materials are not able to reach the glassy state [2]. Both questions are interrelated. To make a glass, it must be cooled fast enough to avoid crystallization, but there is a minimal cooling speed for doing this. For low velocities, the system relaxes toward the most stable configuration: the crystal. The behavior of the viscosity near the glass transition is an important feature of the associated phenomenology and is known in the field as fragility [4–6]. Fragility is related to the glass-forming tendency, since a nonfragile glass former (known as a strong glass former) does not require a fast cooling speed. The viscosity behavior can be changed from strong to fragile by doping [6]. There are many theories available in the field of glasses, but most of them are not able to predict the wide phenomenology observed. For example, it is known that all glasses present anomalies in the density of low-frequency vibrational modes (LFVMs). The most famous one is the boson peak [7], but

there are others, like the floppy-mode contribution, due to the flexible and rigid character of the atomic network [8–10]. Surprisingly, most of the theories concerning the glass transition do not give special importance to the presence of LFVMs. This situation is surprising because for crystals, as shown by Peierls in 1935, thermal stability depends upon LFVMs [7].

In a series of previous papers [11,12], we have shown that the anomalies in the density of LFVMs are a determinant for the glass transition temperature ( $T_g$ ). The key idea was to combine rigidity theory (RT) with the Lindemann criteria for the quadratic mean displacement [11]. Rigidity theory, introduced in this area by Phillips [8] and Thorpe [9], was a major step to understand glass formation. By considering covalent bonding as a mechanical constraint, the ease of glass formation is related to the ratio between the available degrees of freedom and the number of constraints. When the number of constraints is lower than the degrees of freedom, there are nearly zero-frequency vibrational modes called floppy modes [13]. The resulting network is underconstrained. A transition to a rigid lattice occurs by adding bonds. Glasses near the flexible-to-rigid transition are easy to form [8]. Many interesting features of this transition have been experimentally observed, including a self-organized intermediate phase with zero internal stress which shows no-aging [14–16]. Rigidity provides a unique opportunity for tuning the number of LFVMs by chemical doping and thus to observe the resulting consequences in the physical properties [17–19]. For example, Se is a fragile glass that follows a Vogel-Fulcher-Tammann law [6]. It must be cooled very fast

\*On leave from: Departamento de Física-Química, Universidad Nacional Autónoma de México (UNAM), Apartado Postal 20-364, 01000, Distrito Federal, Mexico

to obtain the glass. When doped with other elements like Ge and Se, the average connectivity of the network is increased, and as a result, the glass becomes strong and can be formed even by very slow cooling [6]. However, even if it is believed that RT plays a role in this minimal cooling speed [8], up to now is not clear what the mechanism is behind this observation [20–22]. In this article, we make an exploration of such problem by following a reductionist strategy. In particular, we discuss what are the effects of having an excess of LFVMs in the thermal relaxation properties of simple models of glasses. This thermal relaxation is fundamental to understand how fast thermal equilibrium is achieved and thus how far from equilibrium is the glass. Usually, in the formation of glasses, two kinds of relaxations occur: the  $\beta$  (fast) and  $\alpha$  (slow) relaxation [2]. The fast decay is related to local atomic rearrangements, while the  $\alpha$  relaxation is related to conformational changes that involve tens of atoms [4]. Both are important to the fate of a supercooled liquid, since if a liquid can be prevented from crystallizing down to a temperature at which the time for molecular rearrangement becomes comparable to the experimental time scale, it appears structurally arrested [4]. In the present work, we are interested in how thermal energy is stored in the glass, since such energy is needed in order to produce rearrangements by jumping over potential barriers. Notice that our results are relevant for the size of the time scale of the  $\beta$  relaxation, since here we do not consider rearrangements.

An alternative point of view consists in observing that according to rigidity theory, elastic energy can be stored in each extra bond (constraint) to jump energetic barriers and thus leads to an increased tendency for crystallization. In our model, the addition of constraints is given by second-neighbor springs. Also, as is clear in a supercooled liquid or glass, an external thermal bath removes heat from the system, and in fact, the fate of a supercooled liquid depends upon the rapid conduction of any excess of stored elastic energy to the bath in order to avoid crystallization. Here relaxation is studied by adding a damping term which plays the role of an external bath, and thus the present study provides a link between how elastic energy is stored and conducted through a system depending on the number of anomalies in the LFVMs. It is worthwhile mentioning that although our results are mainly valid for glasses, since the equilibrium positions of the atoms are fixed, they give clues about the thermal relaxation of supercooled liquid near the glass transition at short time scales compared with the  $\alpha$  relaxation. In other words, here we are looking at the fast relaxation around a given inherent structure of the supercooled fluid energy landscape [5].

As pointed out many years ago by Fermi, Pasta, and Ulam [25], the study of thermal relaxation requires the use of nonlinear Hamiltonians. The first attempt to study such processes was the so-called Fermi-Pasta-Ulam (FPU) model of a one-dimensional chain with nonlinear interaction [23–26]. It is amazing that there are still many unsolved questions concerning this simple model [27]. After years of research, it became more or less clear that relaxation is dominated mainly by LFVMs [28–31], due to their quasisonant nature [28]. As a result, they share energy in an efficient way [31] when compared with high-frequency modes. In this article,

we propose to join the study of nonlinear Hamiltonians with the anomalies in LFVMs of glasses, in order to get an insight about how fast a glass relaxes. Thus, here we will study how relaxation is affected by changing the density of LFVMs, as well as the localization properties of the vibrational modes.

The structure of the article is the following. In Sec. II we propose simple models with different densities of LFVMs following the ideas of RT. Then in Sec. III we explain how thermalization was achieved in the simulations, while in Sec. IV we present the results. Finally, Sec. V is devoted to giving some conclusions and perspectives of the present work.

## II. MODELS OF GLASSES

As a starting point, we will formulate a suitable model to study the role of LFVMs and bond constraints. The most simple idea is to modify the FPU model to allow changes at will in the number of LFVMs. The FPU model is a nonlinear Hamiltonian defined in a one-dimensional lattice made of equal masses ( $m$ ) joined by equal springs constants,

$$H = \sum_{j=1}^N \left[ \frac{p_j^2}{2m} + \frac{k}{2}(u_{j+1} - u_j)^2 + \frac{k'}{4}(u_{j+1} - u_j)^4 \right], \quad (1)$$

where  $u_j$  is the displacement of the mass  $m$  at site  $j$  and  $N$  is the number of sites.  $k$  is the harmonic spring constant, and  $k'$  is the strength of the nonlinear interaction. In what follows, we set  $m=1.0$ , and since we are dealing with a system in a finite volume, fixed-end boundary conditions ( $u_0=u_{N+1}=0$ ) are used. The resulting equations of motion are

$$\begin{aligned} \frac{d^2 u_j}{dt^2} = & k(u_{j+1} - u_j) - k(u_j - u_{j-1}) + k'(u_{j+1} - u_j)^3 \\ & - k'(u_j - u_{j-1})^3. \end{aligned} \quad (2)$$

When the anharmonic term  $k'$  is small compared with  $k$ , there are transitions between normal modes of the pure harmonic Hamiltonian, plus a shifting of the eigenfrequencies [32]. Also, discrete breathers appear [27]. As was shown in Refs. [28–33], LFVMs are the ones that mainly influence thermal relaxation. The actual number of LFVMs depends on the structure of the pure harmonic Hamiltonian, since using the rotating phase approximation for small  $k'$ , one can show that the effect of nonlinearity is a shift of the modes toward higher frequencies [32]. Thus, one needs to change the basic structure of the pure harmonic Hamiltonian. This can be done by following the original idea of RT, in which each bond can be treated as a constraint [8,9]. By comparing the number of constraints with the number of degrees of freedom, one can get the fraction of modes with zero frequency, denoted by  $f$ . In the case of a linear chain, the degrees of freedom are  $N$ , while the number of bonds is also  $N$ . This means that there are no floppy modes. Removing bonds does not lead to a flexible lattice, since the lattice is separated in pieces. The only possibility is to add constraints to the system in such a way that the number of LFVMs is reduced with respect to the FPU model. The most simple way to achieve this goal is to add new springs that connect second neighbors [we denote these new springs as second-neighbor

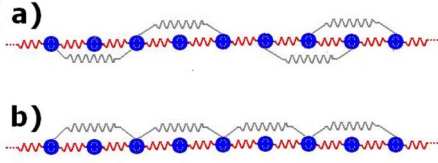


FIG. 1. (Color online) (a) A glass model that has disorder in the SNS connectivity. (b) A modified model that has the same concentration of SNSs as that in (a), but disposed in a periodic arrangement.

springs (SNSs)], as shown in Figs. 1(a) and 1(b). The concentration of such springs is given by  $c$  and is defined as the numbers of SNSs divided by  $N$ . These new springs can be placed at random, as shown in Fig. 1(a) or, in a periodic way, in Fig. 1(b). The Hamiltonian can be written as

$$H = \sum_{j=1}^N \left[ \frac{p_j^2}{2m} + \frac{k}{2}(u_{j+1} - u_j)^2 + \frac{k'}{4}(u_{j+1} - u_j)^4 \right] + \sum_{j=1}^N \Theta_{j+2,j} \left[ \frac{k_2}{2}(u_{j+2} - u_j)^2 + \frac{k'_2}{4}(u_{j+2} - u_j)^4 \right], \quad (3)$$

where  $\Theta_{j+2,j}$  is a random variable that takes the value 0 or 1 with probability  $c$  and  $1-c$ , respectively. Eventually, for comparison purposes, we will use a periodic function for  $\Theta_{j+2,j}$ .

If we consider the pure harmonic case ( $k'=0$  and  $k'_2=0$ ), the number of LFVMs changes as  $c$  goes from 0.0 to 1.0. There are many ways to prove this. First we notice that the limiting cases  $c=0.0$  and  $c=1.0$  are just periodic chains. For  $c=0.0$ , the dispersion relationship is  $\omega(q) = \sqrt{2k[1 - \cos(q)]}$ , where  $q$  is the wave vector and  $\omega(q)$  the corresponding frequency. Using that the density of modes  $\rho(\omega)$  in one dimension is given by [34]

$$\rho(\omega) = \frac{1}{\pi} \left| \frac{dq}{d\omega(q)} \right| \quad (4)$$

and that for the acoustic region  $q \rightarrow 0$ ,  $\omega(q) = qv_{c=0}$ , where  $v_{c=0} = \sqrt{k}$  is the speed of sound for  $c=0$ , it follows that for LFVMs  $\rho_{c=0}(\omega) \approx 1/\pi v_{c=0}$ . Notice that the subscript in  $\rho(\omega)$  indicates the concentration of SNSs. When  $c=1.0$ , it is easy to prove that

$$\omega(q) = \sqrt{2[k + k_2 - k \cos(q) - k_2 \cos(2q)]}, \quad (5)$$

which leads to the result  $\rho_{c=1}(\omega) \approx 1/\pi v_{c=1}$  with  $v_{c=1} = \sqrt{k+4k_2}$ . To treat other cases, we obtained the density of states by diagonalizing the dynamical matrix for chains with  $N=20\,000$  and over an average of 100 disorder realizations, where disorder means here different initial random distributions of second-neighbor springs. For all cases, it was obtained that  $\rho_c(\omega)$  does not depend on  $\omega$  in the low-frequency region. Since  $\rho_c(\omega)$  is a constant for  $\omega \rightarrow 0$ , we can define it as

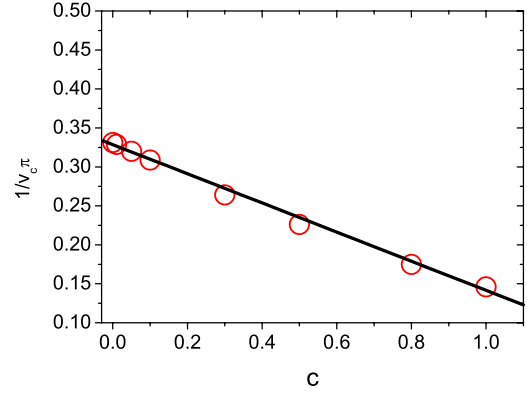


FIG. 2. (Color online) Limiting value of  $\rho_c(\omega)$  as  $\omega \rightarrow 0$  for different concentrations  $c$  of second-neighbor springs. The circles are the results obtained by diagonalizing the Hamiltonian for a chain with  $N=20\,000$  sites, averaged over 100 realizations of disorder. The solid line is a fit with a linear equation.

$$\lim_{\omega \rightarrow 0} \rho_c(\omega) \equiv \frac{1}{\pi v_c}. \quad (6)$$

In Fig. 2 we present a plot of  $1/v_c \pi$  obtained from the simulations. It can be seen that  $1/v_c$  is a linear function that interpolates between  $\rho_{c=1}(\omega)$  and  $\rho_{c=0}(\omega)$ . Such a result is clear since in the limit  $q \rightarrow 0$ , the system can be treated as a continuous medium [35]. Thus, in the proposed model for the harmonic contribution, the density of LFVMs decreases as a function of the concentration  $c$ .

### III. THERMALIZATION OF THE GLASSES

To study the dynamics of the relaxation, first we thermalized the systems by using a bath. Afterwards, the bath was retired and a damping term was added at the ends of the chains to observe the energy dissipation. These steps were made for harmonic and nonharmonic Hamiltonians in order to compare the results. For the case of harmonic Hamiltonians, the systems were prepared in such a way that each normal mode had an energy  $k_B T/2$ , where  $k_B T$  is the temperature measured and  $k_B$  the Boltzmann constant. For nonlinear Hamiltonians, we used a Langevin dynamics in which a stochastic force [ $\eta(t)$ ] and a damping were added to the equation of motion:

$$\frac{d^2 u_j}{dt^2} = - \frac{\partial H}{\partial u_j} - \gamma_0 \frac{du_j}{dt} + \eta_j(t).$$

As usual, the force had a Gaussian distribution, with zero mean  $\langle \eta_i(t) \rangle = 0$  and correlation given by

$$\langle \eta_i(t) \eta_i(t') \rangle = 2\gamma_0 k_B T \delta(t - t'), \quad (7)$$

where  $\gamma_0$  is the damping amplitude.

In all the cases, these equations were solved by using a fourth-order Runge-Kutta algorithm, with parameters such that  $\gamma_0 < 8\pi^2 k/N^2$  (see below) and  $0.0 \leq T \leq 1.0$ . Notice that  $k_B$  was set to 1.0 in all simulations, so  $T$  always has energy units. For validating the software and to test the thermal equilibrium, we performed several tests, including various

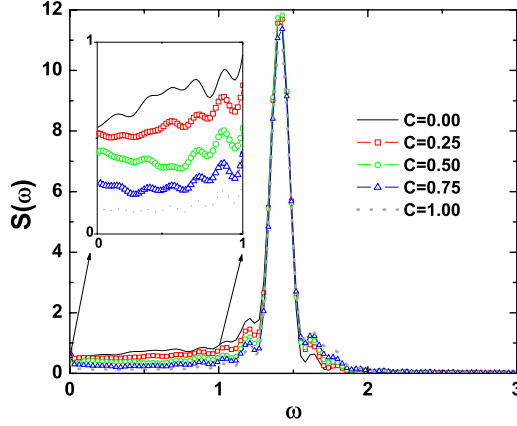


FIG. 3. (Color online)  $S(\omega)$  using a pure harmonic Hamiltonian for different concentrations of SNSs. The inset depicts the low-frequency region, showing the decreasing number of states as a function of  $c$ . The spectra have been obtained using  $N=100$ ,  $T=0.5$ , and  $dt=0.01$ . In this case, the interactions are  $k=k_2=0.5$  and  $k'=k_2=0.0$ . Each curve is an average over ten disorder realizations.

limiting cases. For the linear Hamiltonians, the phonon dynamics was compared with results obtained from other methods. The achievement of thermal equilibration was determined by monitoring the total energy  $E(t)$  as a function of time and the amount of energy in each normal mode. Also, for the harmonic chains we have checked that the kinetic and potential energies of the atoms were fluctuating around  $k_B T/2$ , as expected from the equipartition theorem in thermal equilibrium. Finally, we characterized our systems by looking at the frequency spectrum  $S(\omega)$  of the correlation function when thermal equilibrium is achieved,

$$S(\omega) = 2 \int_0^\infty C(\tau) \cos(\omega\tau) d\tau, \quad (8)$$

where the time correlation  $C(\tau)$  is defined as [30]

$$C(\tau) = \frac{1}{N-1} \sum_{j=2}^N \langle \Delta_j(t+\tau) \Delta_j(t) \rangle \quad (9)$$

and  $\Delta_j(t)$  is the relative displacement:

$$\Delta_j(t) \equiv u_j(t) - u_{j-1}(t) \quad (10)$$

For a pure harmonic Hamiltonian,  $S(\omega)$  can be computed analytically,

$$S(\omega) = \frac{4\gamma_0 k_B T}{N} \sum_{q=0}^{N-1} \frac{1}{[r_1^2(q) + \omega^2][r_2^2(q) + \omega^2]}, \quad (11)$$

where  $r_{1,2}(q)$  are conjugated roots of the secular equation obtained when diagonalizing the Hamiltonian. For a periodic chain, such roots are easily obtained:

$$r_{1,2}(q) = -\frac{\gamma_0}{2} \pm \sqrt{\left(\frac{\gamma_0}{2}\right)^2 - 4k \sin^2\left(\frac{\pi q}{N}\right)}. \quad (12)$$

In Fig. 3,  $S(\omega)$  is shown for chains with different concentrations of SNSs using a pure harmonic Hamiltonian, while in Fig. 4 the same calculation was repeated considering a non-

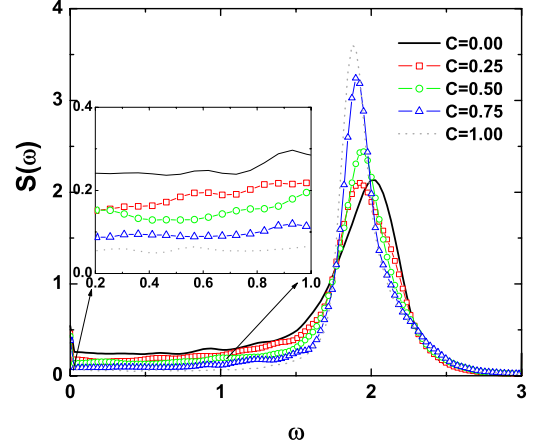


FIG. 4. (Color online)  $S(\omega)$  using a nonlinear Hamiltonian for different concentrations of SNSs. The inset depicts the low-frequency region. The spring constants are shown inside the graph. The spectra have been obtained using  $N=100$ ,  $T=0.5$ , and  $dt=0.01$ . In this case, the interactions are  $k=k_2=0.5$  and  $k'=k_2=0.5$ . Each curve is an average over ten disorder realizations.

linear interaction. In both cases, the temperature was  $T=0.5$  and the time step  $dt=0.01$ . The damping constant  $\gamma_0$  was taken as  $\gamma_0 < 8\pi^2 k/N^2$  in such a way that  $r_{1,2}(q)$  has imaginary roots for the largest separation between eigenfrequencies, avoiding a cutoff effect in  $S(\omega)$  for LFVMs. For all harmonic cases, we have verified that the  $S(\omega)$  calculated from the Runge-Kutta method and from a direct diagonalization using Eq. (11) are in complete agreement. In Figs. 3 and 4, we include a close-up of the low-frequency region, showing that  $S(\omega)$  is reduced for small  $\omega$  with increasing  $c$ , as expected.

#### IV. ENERGY RELAXATION AND LOW-FREQUENCY MODES

The relaxation of the thermalized models from an initial temperature  $T$  to zero temperature has been studied following two steps: first the thermal bath was retired and then a damping term was added at both ends of the chains. The resulting equations of motion are

$$\frac{d^2 u_j}{dt^2} = -\frac{\partial H}{\partial u_j} - \sum_{j=1}^N \Gamma_{jl} \frac{du_j}{dt}, \quad (13)$$

where  $\Gamma_{jl}$  is the dissipation near the ends of the chain,

$$\Gamma_{jl} = \gamma \delta_{jl} [\delta_{j,1} + \delta_{j,N}], \quad (14)$$

$\gamma$  is the damping constant, and  $\delta_{jl}$  is a Kronecker delta. For all chains we took  $\gamma = \gamma_0$ .

In Figs. 5 and 6 we present a plot of the energy relaxation using nonlinear Hamiltonians for different concentrations of SNSs. Notice that in Fig. 5 we present the evolution from  $c=0.0$  to  $c=0.5$ , while in Fig. 6 the concentration goes from  $c=0.5$  to  $1.0$ . This separation was made in order to simplify the discussion of the results. Each of the plots for the energy relaxation was made for  $N=100$ , starting from thermalized baths at  $T=0.5$ . An average over 40 disorder realizations was made in all cases.



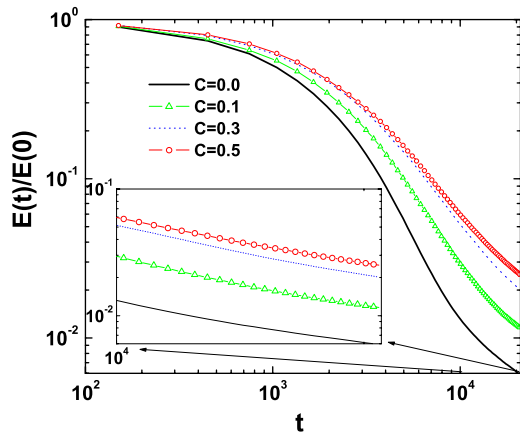


FIG. 5. (Color online) Energy relaxation as a function of time for  $c=0-0.5$  using a nonlinear Hamiltonian with parameters  $k=k_2=0.5$  and  $k'=k'_2=0.5$ . The inset shows a close-up of the relaxation tail. For all chains,  $N=100$  and  $dt=0.01$ , and an average over 40 disorder realizations was made. The initial temperature is  $T=0.5$ .

There are many interesting features in the plots of the relaxation. The first one is that the time required for relaxation increases as  $c$  goes from  $c=0.0$  to  $0.5$ . From  $c=0.5$  to  $1.0$ , this behavior is reversed for  $t \leq 10^4$ , since the time required for relaxation decreases with  $c$ . Near the crossover time  $t \approx 10^4$ , the relaxation becomes slow as the concentration of SNSs is increased. At  $c=1.0$ , the slowest relaxation is observed. Thus we can conclude that for long times, relaxation is always slow when the number of LFVMs is reduced. This long-time behavior can be understood in terms of the depletion of LFVMs, as was explained in the Introduction. According to Ref. [30], the relaxation of high-frequency modes requires a transference of energy to LFVMs. Such a phenomenon is akin to turbulence [31], in which energy is injected at large scales and transferred via a cascade of self-similar eddies to a small scale in which energy is finally dissipated. In the present case, the reduction of LFVMs

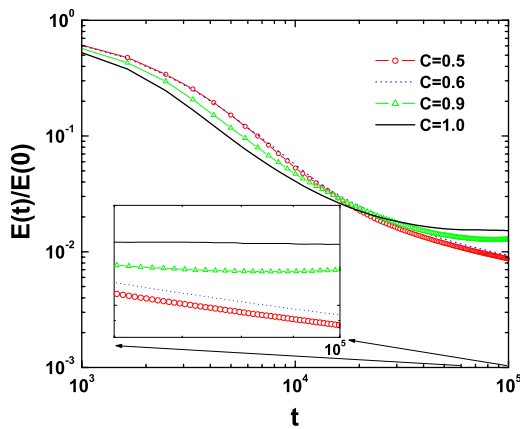


FIG. 6. (Color online) Energy relaxation as a function of time for  $c=0.5-1.0$ . The inset shows a close-up of the relaxation tail. For all chains,  $N=100$  and  $dt=0.01$ , and an average over 40 disorder realizations was made. The interactions are  $k=k_2=0.5$  and  $k'=k'_2=0.5$ . The initial temperature is  $T=0.5$ .

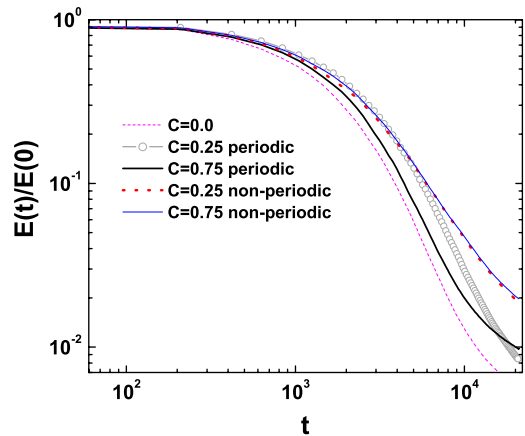


FIG. 7. (Color online) Energy relaxation of several concentrations and lattice topologies for a nonlinear Hamiltonian with parameters  $k=k_2=0.5$  and  $k'=k'_2=0.5$ . The other parameters of the simulations were the same as those in the previous plots.

means that no so many modes are available to dissipate energy. As a result, energy relaxation is slower.

In spite of this, our results show that this is not the only effect. The density of LFVMs decreases from  $c=0.0$  to  $1.0$ , while the time required for thermal relaxation in disordered chains has a maximum around  $c=0.5$  for times  $t < 10^4$ . This fact means that the transference toward LFVMs is not the only factor that determines thermal relaxation. To clarify this point, we decided to compare disordered chains with periodic chains that contained the same concentration of SNSs. An example of a periodic lattice with a certain concentration of SNSs was already given in Fig. 1. In Fig. 7 we present some interesting cases, such as the relaxation of the periodic cases  $c=0.25$  and  $0.75$ .

From Fig. 7, it is clear that around  $t=2.0 \times 10^4$ , the periodic array with  $c=0.75$  begins to relax slower than the  $c=0.25$  case. This is a clear indication that the depletion of LFVMs produces a slow relaxation for very long times, as expected from the arguments of energy sharing. We can see in Fig. 7 that the disordered cases  $c=0.75$  and  $0.25$  relax in a very similar way before the crossover. Since both contain different numbers of LFVMs, but almost the same degree of disorder when compared to  $c=0.0$  and  $1.0$ , we can conclude that for these concentrations and time scale, the spatial shape of the normal modes seems to be as important as the number of LFVMs in the disordered chain. Although for a given concentration of SNSs a disordered and a periodic chain have nearly the same density of normal modes for LFVMs (below the Ishii limit [37]), for the pure harmonic disordered cases the high-frequency normal modes are localized. As a result, energy is not transferred so fast to the LFVMs. However, the periodic cases  $c=0.25$  and  $0.75$  show that in the long-term behavior, the absence of LFVMs is fundamental. This long-trend behavior is very clear for the case  $c=1$  which deserves a special mention, since although it relaxes very similarly to the  $c=0.0$  case at small times, at  $t \approx 10^4$  it begins to relax more slowly than any other curve.

In Fig. 8 we present another comparison of the relaxation for a periodic and a disordered chain with  $c=0.5$ . One can clearly see how the nonperiodic array relaxes more slowly

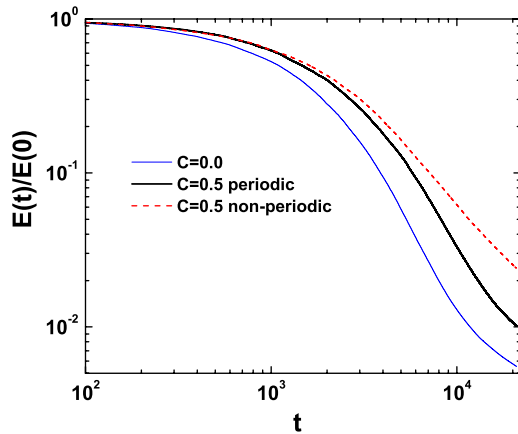


FIG. 8. (Color online) Energy relaxation as a function of time for the cases  $c=0.0$ ,  $0.5$  periodic, and  $0.5$  nonperiodic using a nonlinear Hamiltonian with parameters  $k=k_2=0.5$  and  $k'=k'_2=0.5$ . Notice how the disordered case relaxes slower than the periodic case. The other parameters used in the simulations were the same as those in the previous plots.

than the periodic array. In both cases, the relaxation is slower than the  $c=0.0$  case. From this discussion, it is possible to conclude that the localization of normal modes, due to disorder, plays a role in the relaxation time.

It is worthwhile mentioning that one must not be confused by the term “localization.” In the previous discussion, the term localization referred to the normal-mode characteristics of the associated harmonic problem—i.e., when  $k' \rightarrow 0$ . Such localization is a consequence of disorder. There is another kind of localization due to the existence of breathers [29], which is basically a purely nonlinear effect. To understand this, we calculated the energy localization parameter  $\mathcal{L}(t)$ , defined as [36]

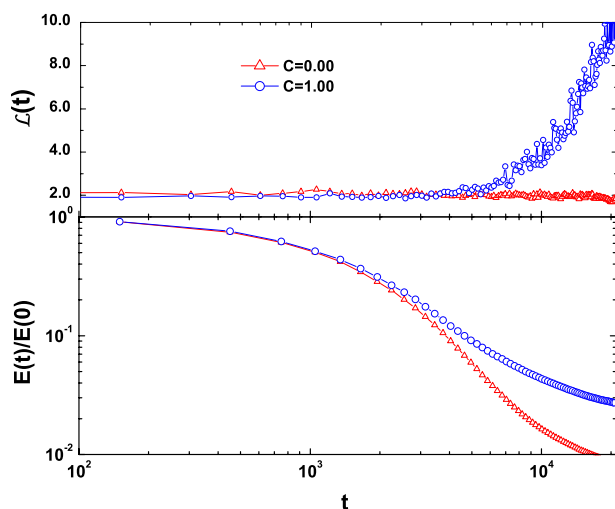


FIG. 9. (Color online) Comparison between the localization of energy and relaxation for the nondisordered cases  $c=0.0$  and  $1.0$ . Notice that the case  $c=1.0$  contains fewer LFVMS, and as a result, relaxation is slower. The parameters used were  $N=100$  and  $dt=0.01$  with parameters  $k=k_2=0.5$  and  $k'=k'_2=0.5$ .

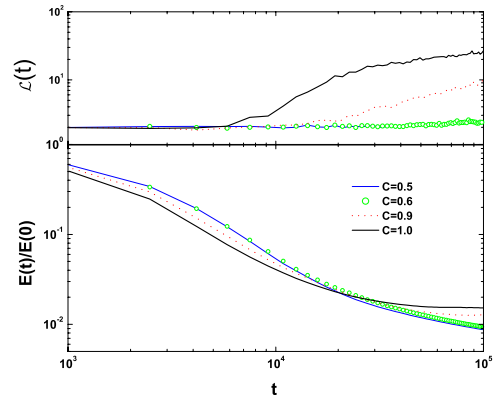


FIG. 10. (Color online) Energy localization for different concentrations  $c$  compared with the energy relaxation using disordered chains. The parameters used were  $N=100$  and  $dt=0.01$  with parameters  $k=k_2=0.5$  and  $k'=k'_2=0.5$ . An average over 40 realizations of disorder was made.

$$\mathcal{L}(t) = \frac{\sum_{j=1}^N e_j^2(t)}{[\sum_{j=1}^N e_j(t)]^2},$$

where  $e_j(t)$  is the energy localized in a given site:

$$e_j(t) = \left[ \frac{p_j^2}{2m} + \frac{k}{2}(u_{j+1} - u_j)^2 + \frac{k'}{4}(u_{j+1} - u_j)^4 \right] + \Theta_{j+2,j} \left[ \frac{k_2}{2}(u_{j+2} - u_j)^2 + \frac{k'_2}{4}(u_{j+2} - u_j)^4 \right].$$

The role of the parameter  $\mathcal{L}(t)$  is to give a rough estimate on how energy is localized in the chain. In Fig. 9 we compare  $\mathcal{L}(t)$  for the cases  $c=0.0$  and  $1.0$ . Clearly, for times  $t > 10^4$  the energy begins to be much more localized in the case  $c=1$ , due to the depletion of LFVMS, compared to  $c=0.0$ . In Fig. 9, the relaxation behavior is presented for comparison, showing that the slow-relaxation properties are due to the energy localization since both chains are periodic. As a consequence, if  $k' \rightarrow 0$ , both chains present nonlocalized normal modes. In fact, it is easy to prove that for  $k'=0$ , the chains with  $c=0.0$  and  $1.0$  relax at the same time.

In Fig. 10, we show a plot of the energy relaxation and localization for  $c=0.5-1.0$  using nonlinear chains. One can observe the relationship between energy localization and relaxation due to nonlinear effects, since the case  $c=1.0$  does not contain disorder as in the cases  $c=0.5, 0.6$ , and  $0.9$ .

### V. CONCLUSIONS

The present study shows that low-frequency modes have a great impact on thermal relaxation. Such impact not only arises as a consequence of the cascade mechanism that dissipates energy from high- to low-frequency modes, but also because of the interplay between localization and nonlinearity. A decrease in the number of low-frequency vibrational modes leads to an increased relaxation time on a small scale compared with the structural rearrangement time scale. It is worthwhile mentioning that our results are in complete

agreement with the idea of Phillips that the cooling speed is related to the number of constraints (bonds) [8]. Here we proved that such an effect is not only due to the extra stored elastic energy, but also to the fact that energy cannot be transmitted in an efficient way to the thermal bath due to a depletion of vibrational modes in the low-frequency region. In fact, such phenomena can be also explained in terms of the energy landscape curvature in the direction of floppy modes [12,22]. This work suggests that experiments be performed to look for an increased time scale for thermal relax-

ation and a decreased thermal conductivity when the number of low-frequency modes is reduced. Such a study can be made in a systematic way by doping chalcogenide glasses to change the connectivity of the network.

#### ACKNOWLEDGMENTS

We thank DGAPA-UNAM Projects No. IN-117806 and No. IN-111906 and CONACyT Grants No. 48783-F and No. 50368 for financial support.

- 
- [1] P. W. Anderson, *Science* **267**, 1615 (1995).  
 [2] J. Jackle, *Rep. Prog. Phys.* **49**, 171 (1986).  
 [3] J. C. Phillips, *Rep. Prog. Phys.* **59**, 1133 (1996).  
 [4] P. G. Debenedetti, *Metastable Liquids* (Princeton University Press, Princeton, 1996).  
 [5] P. G. Debenedetti and F. H. Stillinger, *Nature (London)* **410**, 259 (2001).  
 [6] M. Tatsumisago, B. L. Halfpap, J. L. Green, S. M. Lindsay, and C. A. Angell, *Phys. Rev. Lett.* **64**, 1549 (1990).  
 [7] K. Binder and W. Kob, *Glassy Materials and Disordered Solids* (World Scientific, Singapore, 2005).  
 [8] J. C. Phillips, *J. Non-Cryst. Solids* **34**, 153 (1979).  
 [9] M. F. Thorpe, *J. Non-Cryst. Solids* **57**, 355 (1983).  
 [10] J. C. Phillips, in *Rigidity Theory and Applications*, edited by M. Thorpe and P. M. Duxbury (Kluwer Academic, New York, 1999).  
 [11] G. G. Naumis, *Phys. Rev. B* **73**, 172202 (2006).  
 [12] G. G. Naumis, *J. Non-Cryst. Solids* **352**, 4865 (2006).  
 [13] H. He and M. F. Thorpe, *Phys. Rev. Lett.* **54**, 2107 (1985).  
 [14] D. Selvanathan, W. J. Bresser, and P. Boolchand, *Phys. Rev. B* **61**, 15061 (2000).  
 [15] P. Boolchand, in *Insulating and Semiconducting Glasses*, edited by P. Boolchand (World Scientific, Singapore, 2000).  
 [16] Y. Wang, J. Wells, D. G. Georgiev, P. Boolchand, K. Jackson, and M. Micoulaut, *Phys. Rev. Lett.* **87**, 185503 (2001).  
 [17] P. Lucas, E. A. King, A. D. Horner, and S. K. Sundaram, *J. Non-Cryst. Solids* **352**, 2067 (2006).  
 [18] P. Lucas, *J. Phys.: Condens. Matter* **18**, 5629 (2006).  
 [19] P. Boolchand, D.G. Georgiev, T. Qu, F. Wang, L. Cai, and S. Chakravarty, *C. R. Chim.* **5**, 713 (2002).  
 [20] G. G. Naumis, *Phys. Rev. B* **61**, R9205 (2000).  
 [21] A. Huerta and G. G. Naumis, *Phys. Rev. Lett.* **90**, 145701 (2003).  
 [22] G. G. Naumis, *Phys. Rev. E* **71**, 026114 (2005).  
 [23] A. Huerta and G. G. Naumis, *Phys. Lett. A* **299**, 660 (2002).  
 [24] A. Huerta and G. G. Naumis, *Phys. Rev. B* **66**, 184204 (2002).  
 [25] E. Fermi, J. Pasta, and S. Ulam, *Enrico Fermi, Collected Papers II*, edited by E. Segre (University Chicago Press, Chicago, 1965).  
 [26] M. Toda, *Theory of Non-Linear Lattices* (Springer-Verlag, Berlin, 1988).  
 [27] D. K. Campbell, S. Flach, and Y. S. Kivshar, *Phys. Today* **57**(1), 43 (2004).  
 [28] J. Ford, *J. Math. Phys.* **2**, 387 (1961).  
 [29] R. Reigada, A. Sarmiento, and K. Lindenberg, *Phys. Rev. E* **63**, 066113 (2001).  
 [30] R. Reigada, A. Sarmiento, and K. Lindenberg, *Phys. Rev. E* **64**, 066608 (2001).  
 [31] A. Ponomarev, in *Chaotic Dynamics and Transport in Classical and Quantum Systems*, Proceedings of the NATO Advanced Study Institute on International Summer School on Chaotic Dynamics and Transport in Classical and Quantum Systems Cargèse, Corsica, 2003, edited by P. Collet, M. Courbage, S. Metens, A. Neishtadt, and G. Zaslavsky, (Springer, Amsterdam, 2005), Vol. 182, p. 431.  
 [32] I. Limas, G. G. Naumis, F. Salazar, and C. Wang, *Phys. Lett. A* **337**, 141 (2005).  
 [33] R. Reigada, A. Sarmiento, and K. Lindenberg, *Phys. Rev. E* **66**, 046607 (2002).  
 [34] N. W. Ashcroft and N. D. Mermin, *Solid State Physics* (Saunders College, Philadelphia, 1976).  
 [35] S. Lepri, R. Livi, and A. Politi, e-print arXiv:cond-mat/0112193.  
 [36] F. Piazza, S. Lepri, and R. Livi, *J. Phys. A* **34**, 9803 (2001).  
 [37] H. Matsuda and K. Ishii, *Prog. Theor. Phys. Suppl.* **45**, 56 (1970).